

Two-Dimensional Optimal Power Map Generation through Minimum Variance Estimation Technique

Je Heon Bang^{a*}, Ho Chul Shin^b, Sun Kwan Hong^b, John C. Lee^{a,c}

^aDepartment of Advanced Nuclear Engineering, POSTECH, Pohang 790-784, Korea

^bKorea Hydro and Nuclear Plant-Central Research Institute, Yuseon-gu 305-340, Daejeon, Korea

^cDepartment of Nuclear Engineering, University of Michigan, Ann Arbor, Michigan, USA

*Corresponding author: jhbang@postech.ac.kr

1. Introduction

The power peaking factor representing a ratio of the maximum to average power densities in the core is one of the key parameters that determine the power rating of a nuclear power plant (NPP). Conventional methods for generating the power map involve the use of the calculated power distribution to interpolate incore detector reaction rates in instrumented assemblies with nominal power-to-signal ratios [1]. Measurement uncertainties and parametric variations in the calculated power distribution are then represented via the uncertainty hot channel factor F_q^U and the engineering hot channel factor F_q^E to arrive at the overall hot channel factor F_q [2,3]. We developed a Kalman filtering minimum-variance estimation (MVE) technique [4,5] that represents uncertainties in measured detector signals and predicted power distribution directly to determine an optimal power distribution. This paper presents the application of the MVE method to determine an optimal 2-D power distribution in a PWR core.

2. Kalman filtering MVE model

For 157 fuel assemblies in the core, a 314-dimensional state vector \mathbf{x} is set up to represent the two-group flux distributions in the core. The posterior state vector \mathbf{x}^+ , after measurements, is obtained from the prior distribution \mathbf{x}^- accounting for random fluctuations

$$\mathbf{x}^+ = \mathbf{x}^- + \mathbf{w}, \quad (1)$$

where \mathbf{x}^- is generated from a 3-D nodal diffusion theory calculation with the ANC code [6] and \mathbf{w} is a white Gaussian distribution with covariance \mathbf{Q} . The 3-D incore detector signals are averaged along the length of the fuel assemblies to obtain 2-D reaction rates in the 157-dimensional measurement vector \mathbf{z} representing the normalized assembly power distribution obtained with the INCORE code [1]:

$$\mathbf{z} = \mathbf{H}\mathbf{x} + \mathbf{v}, \quad (2)$$

where \mathbf{H} is the measurement transformation matrix connecting \mathbf{x} to \mathbf{z} and \mathbf{v} is a white Gaussian distribution with covariance \mathbf{R} .

Once incore measurements are obtained, the posterior flux distribution is obtained to optimally correct for the difference between the measurement \mathbf{z} and prediction $\mathbf{H}\mathbf{x}^-$

$$\mathbf{x}^+ = \mathbf{x}^- + \mathbf{K}(\mathbf{z} - \mathbf{H}\mathbf{x}^-), \quad (3)$$

in terms of the Kalman gain matrix \mathbf{K}

$$\mathbf{K} = \mathbf{P}^- \mathbf{H}^T (\mathbf{H}\mathbf{P}^- \mathbf{H}^T + \mathbf{R})^{-1}. \quad (4)$$

The updated posterior estimate of the covariance for the state vector \mathbf{x}^+ is determined:

$$\mathbf{P}^+ = (\mathbf{I} - \mathbf{K}\mathbf{H})\mathbf{P}^- = \mathbf{E}\{(\mathbf{x} - \mathbf{x}^+)^T(\mathbf{x} - \mathbf{x}^+)\}, \quad (5)$$

where the prior covariance \mathbf{P}^- is set to \mathbf{Q} of Eq. (1). Finally, given the optimal estimate \mathbf{x}^+ for the neutron flux distribution, we may readily calculate the corresponding optimal estimate for the power distribution by $\mathbf{H}\mathbf{x}^+$ and determine the 2-D power peaking factor F_{xy} as the upper bound estimate for the normalized power in the peak power assembly.

3. Numerical results and comparison with conventional power mapping approach

3.1 Estimates for initial covariance matrices

The first step of MVE generates the optimal power map using typical uncertainty value $F_q^U = 1.05$ and $F_q^E = 1.03$ with an upper confidence level of 99.9% corresponding to 3σ values for 3-D power map. For our 2-D power map study, we thus obtain $\sigma_E = 0.7\%$ and $\sigma_U = 1.1\%$ as initial estimates for uncertainties in the system state \mathbf{x} and measurement vector \mathbf{z} . For upper bound estimates, however, we have used 3σ values to compare directly with the $F_q^U = 1.05$ and $F_q^E = 1.03$ for 3-D or $F_q^U = 1.033$ and $F_q^E = 1.020$ for 2-D power maps.

3.2 Test calculation with actual incore measurement

We performed our test calculations for a PWR core at a hot full power condition with all rods out with a power output of 2775 MWt at the burnup step 6544.5 MWD/MTU. Moveable miniature fission chambers are used to obtain reaction rates in 49 assemblies out of a total of 157 assemblies in the core. The optimal power map generated via the MVE technique is shown in Figure 1 together with the ANC prediction power and measured maps obtained through the INCORE code. The optimal power distribution lies mostly close to the ANC power map because $\sigma_E < \sigma_u$, i.e., calculational errors are assumed less than measurement errors in

determining the Kalman gain matrix \mathbf{K} of Eq. (4). In the opposite case, the optimal power distribution would approach the measured power distribution.

0.726	0.928	1.124	1.095	1.328	1.139	1.160	0.386
0.731	0.928	1.124	1.088	1.325	1.141	1.165	0.388
0.730	0.928	1.124	1.090	1.326	1.141	1.164	0.387
0.743	0.945	1.144	1.110	1.349	1.161	1.185	0.395
0.933	1.136	1.068	1.279	1.112	1.329	1.096	0.325
0.928	1.131	1.062	1.269	1.106	1.324	1.095	0.325
0.929	1.132	1.064	1.272	1.108	1.325	1.095	0.325
0.946	1.152	1.083	1.294	1.128	1.349	1.115	0.331
1.132	1.070	1.291	1.135	1.161	1.250	0.643	
1.124	1.062	1.281	1.124	1.151	1.239	0.641	
1.126	1.064	1.284	1.127	1.154	1.242	0.641	
1.146	1.083	1.307	1.147	1.174	1.264	0.653	
1.101	1.282	1.136	1.149	1.323	1.103	0.349	
1.088	1.269	1.125	1.141	1.315	1.095	0.345	
1.092	1.273	1.128	1.143	1.317	1.097	0.346	
1.111	1.295	1.148	1.163	1.340	1.117	0.352	
1.339	1.117	1.161	1.323	1.131	0.534		
1.325	1.106	1.151	1.314	1.124	0.531		
1.329	1.109	1.153	1.316	1.126	0.532		
1.352	1.129	1.174	1.340	1.146	0.541		
1.150	1.330	1.241	1.097	0.533			
1.141	1.324	1.238	1.093	0.530			
1.144	1.325	1.239	1.094	0.531			
1.164	1.349	1.261	1.113	0.540			
1.165	1.100	0.641	0.341				
1.165	1.095	0.639	0.339				
1.165	1.096	0.640	0.339				
1.186	1.116	0.651	0.346				
0.386	0.325						
0.388	0.325						
0.387	0.325						
0.395	0.331						

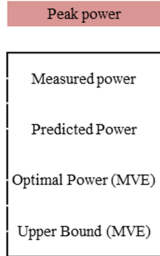


Figure 1. Comparison of 2-D power distributions with $3\sigma_E = 2.0\%$ and $3\sigma_U = 3.3\%$

3.3 Upper bound peaking factor

In the quarter-core power maps compared in Figure 1, we also include upper bound estimate for the MVE power distribution with 3σ estimates of uncertainties. We also show results of parametric studies with varying values of the uncertainties in Table 1.

Table 1: The upper bound power corresponding to 99.9% confidence level

	$3\sigma_E$ (%)	1.0	2.0	3.0	4.0
		$3\sigma_U = 1.5\%$	$F_{xy}(\text{INCORE})$	1.373	1.386
	$F_{xy}(\text{MVE})$	1.340	1.350	1.354	1.356
	% difference	2.4	2.6	3.3	4.0
$3\sigma_U = 3.3\%$	$F_{xy}(\text{INCORE})$	1.397	1.411	1.425	1.439
	$F_{xy}(\text{MVE})$	1.339	1.352	1.361	1.367
	% difference	4.2	4.2	4.5	5.0

* including only signal fluctuations for a calibration thimble without any other uncertainty like tabulated cross-sectional data might be the lowest limit.

Note that for conventional INCORE approach, the 2-D peaking factor $F_{xy}(\text{INCORE})$ simply adds $F_q^U = 1.033$ and $F_q^E = 1.020$ to the peak assembly measured power of 1.339, while $F_{xy}(\text{MVE})$ includes the

3σ equal to 1.9% of \mathbf{P}^+ of Eq. (5). Peak power assembly in Figure 1 and the parametric results in Table 1 both show that $F_{xy}(\text{MVE})$ is less than $F_{xy}(\text{INCORE})$ and less sensitive to σ_E and σ_U . This rather significant result originates from the optimal state estimates provided by the Kalman filter technique, in particular, the posterior covariance matrix of Eq. (5). Substituting the Kalman gain matrix \mathbf{K} of Eq. (4) into Eq. (5), we note that the posterior covariance \mathbf{P}^+ should be smaller than the prior or initial covariance \mathbf{P}^- .

4. Conclusions

Although this study shows the possibilities of reducing the uncertainty and obtaining realistic power maps through the Kalman filter algorithm developed, further studies would be necessary to extend the algorithm to 3-D power map generations. Additional studies would be required to obtain accurate estimate of errors associated with both flux measurements and predictions. This research ultimately aims at representing the evolution of 3-D flux and power distributions over fuel cycles through optimal estimation techniques to obtain more accurate fuel burnup distributions. For this purpose, unscented Kalman filter algorithms [5] should be developed to represent the nonlinear variations of flux distributions as a function of fuel burnup accurately and conveniently. Furthermore, H-infinite filters may be better suited for representing upper bounds since the power mapping algorithm should accommodate conceivable disturbances more systematically [5].

Acknowledgment

This research was supported by WCU (World Class University) program through the National Research Foundation of Korea funded by the Ministry of Education, Science and Technology (R31-30005)

REFERENCES

- [1] "INCORE 3D User manual," Westinghouse Electric Company.
- [2] J. C. Lee, "Nuclear Reactor Physics and Engineering," Unpublished Lecture Note, Department of Advanced Nuclear Engineering, POSTECH (2011).
- [3] J. C. Lee and N. J. McCormick, *Risk and safety analysis of Nuclear System*, Wiley (2011).
- [4] J. W. BRYSON, J. C. LEE, and J. A. Hassberg, "Optimal Flux Map Generation through Parameter Estimation Techniques," *Nucl. Sci. Eng.* **114**, 238 (1993).
- [5] D. Simon, *Optimal State Estimation*, Wiley (2006).
- [6] "ANC User manual," Westinghouse Electric Company.